Chapter 6

Ceramic Foam Composite using Industrial Solid Waste (Coal Overburden) via Sucrose Dehydration process-1

The contents of this chapter have appeared as:

"An economic and sustainable approach to transform aluminosilicate-rich solid waste to functionally graded composite foam for high-temperature applications"

Vaibhav Pandey, Mayank Kumar Yadav, S.K. Panda, V.K. Singh,

Chemosphere 338 (2023) 139588

https://doi.org/10.1016/j.chemosphere.2023.139588

6.1 Introduction

Functionally graded ceramic foam (FGCF), a subclass of functionally graded materials with gradient microstructures, has attracted a lot of research attention as a high-performing engineering material [156]. In comparison to the more widespread use of ceramic foams, the FGCF with pore-gradient continually changing in diameter exhibit enhanced features of reduced filtration resistance and higher separation efficiency [157]. FGCF can be applied in a variety of fields, including insulating refractories, aerospace, biomaterials, supports for ceramic filters, high-temperature insulators and active cooling parts, energy conversion, and more [158,159]. To date, numerous manufacturing processes have been developed to fabricate FGCF, including freeze casting [160], dip coating [161], thermal radiation technique [162] foaming using blowing agent [163], modified sponge replication method [164], additive manufacturing [165] etc. Despite various approaches, there is still a gap in the manufacturing of FGCF, that can offer a one-step processing route along with operational benefits of cheap cost, ease of handling with effective control over materials microstructure, and porosity.

Thus, a straightforward and adaptable method for creating FGCF with gradient microstructure is systematically and comprehensively suggested in the present study. This approach is based on the thermo-foaming effect shown by sucrose-mixed ceramic powders with sulphuric acid. However, exploiting thermo-foaming characteristics to develop porous structures from industrial wastes has never been cited earlier as an effective mass conversion mechanism for availing economically feasible useful products.

Taking note of the concerns associated with solid wastes like MW and the applicability of FGCF structures, the present work is an effort towards a sustainable utilization and recycling of waste by developing functionally graded mullite embedded silicate composite (FG-MS) foam using industrial waste (MW as model solid waste) through an economic thermo-processing technique and finding its application in several cases; one is thermal insulation. The mobility of heavy metals in the leachates of the developed foam is checked according to toxicity characteristic leaching approach (TCLP). The study includes thermomechanical characterization of FG-MS foams fabricated via sucrose dehydration process and compares them with the existing mullite foams prepared through other routes and materials. A cost analysis was also included to evaluate the economic feasibility of the above process.

6.2 Experimental Procedure

6.2.1 Raw Materials

The primary ingredient used for the fabrication of FG-MS foam is MW which is collected from the open-cast mine of Bina site, Northern Coalfield Limited (NCL) Singrauli, India. The collected MW samples were initially air-dried and subsequently grounded to get finer particles and then sieved through a 180-micron-sized sieve and kept for further characterization. Both the sucrose and the concentrated H_2SO_4 (98 wt.%) used are of laboratory research quality (Loba, India).

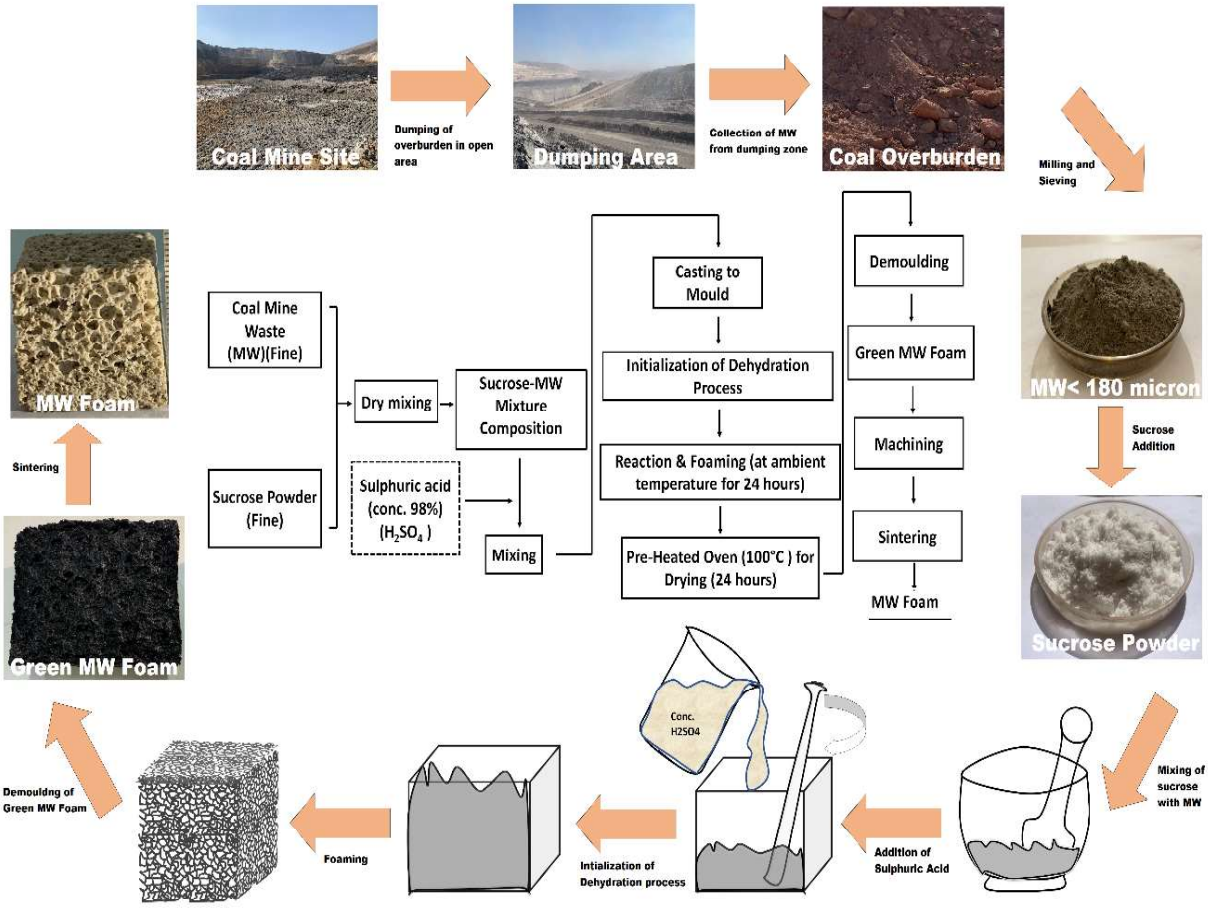

Fig. 6.1 Standard process flow chart of fabrication of FG-MS foam

6.2.2 Fabrication Methodology

The fabrication process of FG-MS foams is based on the dehydration of sucrose with sulphuric acid which helps in foaming of MW. In brief, the sieved MW samples were mixed with finer sucrose powder in a defined concentration, and the optimized amount of sulphuric acid was added to the mixture to get a slurry paste. This slurry was then cast into an appropriate cast and kept in the ambient atmosphere for 24 hours for dehydration reaction and foaming. The foamed

samples were then kept in an oven at 100°C for drying. The dried green foam samples were machined to get proper shape and then kept for the sintering (1300°C-1500°C) process for final consolidation. Fig. 6.1 demarcates the schematic of the fabrication process used to develop the FG-MS foam.

6.2.3 Characterization Techniques

The assessment of the raw MW, green MW foam post-dehydration, and sintered FG-MS foam involves meticulous employment of characterization techniques, as well as adherence to specific standards and procedures outlined in section 5.2.3 of chapter 5. Furthermore, the evaluation of the physical and thermo-mechanical properties of the developed FG-MS foam is conducted following the procedure elucidated in section 5.2.3 of chapter 5.

6.3 Results and Discussion

6.3.1 Characterization of Raw MW

The details of raw MW characterizations with detailed results can be seen from previous chapter (Section 5.3.1, Chapter 5). The comprehensive details regarding the characterizations of the raw MW, along with in-depth results, are available in the preceding chapter, specifically in Section 5.3.1 of Chapter 5.

6.3.2 Synthesis Mechanism, Characterization and Microstructural Evolution of FG-MS Foam

Highly porous mullite-silicate foams with gradient pores were fabricated by realizing reaction generated thermo-foaming process using sucrose as blowing agent and sulphuric acid as dehydrating agent. Initially, optimization of sulphuric acid was achieved through extensive experiments by fixing the sucrose amount and found to be approximately 40 wt% of the powder mixture. Optimization of sulphuric acid amount is based on the requirement of dehydration process to complete the reaction and also to maintain the slurry viscosity which can successfully support foaming phenomenon and foamed structure. When MW-sucrose mixture is treated with optimized amount of sulphuric acid, dehydration of sucrose initiates. Before the start of dehydration reaction, delay in reaction is observed. This delay helps in slurry formation which further promotes proper interaction and adhering of sucrose particles with MW particles. Since MW mostly consists of aluminosilicate minerals, the interaction of the hydroxyl groups in sucrose with the surfaces of silica and alumina particles can also be considered a factor in the adhesion of sucrose particles. Sucrose molecules are broken down into water and carbon molecules when H_2SO_4 reacts with them. The carbon that results, agglutinates on the MW

particles. Additionally, the remaining H_2SO_4 interacts with the carbon to produce the gases sulphur dioxide and carbon dioxide. Due to the exothermic nature of the processes used to hydrate sulphuric acid and dehydrate sucrose, tremendous heat was produced. This heat vaporizes the water molecules, and water vapour along with CO_2 and SO_2 gases starts exerting pressure inside the slurry and escapes out by creating hierarchical porous 3D network of carbon coated FG-MS foam (Fig. 6.3(a)).

The chemical change in the MW-sucrose mixture due to dehydration process is analysed using FTIR analysis (Fig. 6.2(a)) and two additional peaks are found in the green FG-MS foam sample. Peaks at 1639.2 cm^{-1} may mimic C=C stretches, which suggests aromatic groups. One of the O=S=O, -SO_3H group, and Si-OH group vibrations that arise after carbonization and are caused by the esterification and oxidation of the many O-H groups in sucrose by H_2SO_4 may correspond to another peak at 1296.4 cm^{-1}[153]. The dehydration and carbonization processes are approved by the presence of these powerful, sharp peaks. Green foams with varying foam height can be obtained using different sucrose to MW weight ($W_{Su/MW}$) ratio. Fig. 6.2(c) shows effect of $W_{Su/MW}$ ratio on foaming behaviour. Foaming increases with increase in sucrose weight ratio. The weight loss pattern of the green MG-MS foam shows three stages between 0-790°C, there after maintaining constant weight when kept for further heating (Fig. 6.2(d)). In the first cycle (0-380°C), weight loss is steady and is due to the escape of water vapour and oxidation of carbon, with a total weight loss of 14.49 %. The second stage (440-540°C) is comparatively smaller and belongs to the volatilisation of remaining carbon and other organic matter with a total loss of 6.46%. In the last stage, between 620°C and 790°C, weight loss is associated with the removal of SO_2 gases and change and decomposition of the phases of various minerals present in MW. Weight loss in the final stage is very sharp and accounts for a total weight loss of 14.12%. Based on the TGA result, sintering was done at a scheduled heating rate of 3°C/minute up to 800°C to remove all the organic impurities, which is followed by a final consolidation process from 1300°C to 1500°C at 5°C/minute.

Fig. 6.3(b) shows images of FG-MS foams of various compositions obtained after the consolidation process, showing hierarchical pore structure. It is clearly evident from visual images that $W_{Su/MW}$ ratio has a significant influence on the porosity and pore morphology of FG-MS foams. FG-MS foams with higher porosity are obtained at a higher $W_{Su/MW}$ ratio. Due to the complex compositions of raw MW, green FG-MS foams undergo several transformations at high sintering temperatures which also significantly affect the microstructure of the foams. FTIR result highlighted the disappearance of peaks which were aroused due to the

carbonization of green foams. The existence of peaks at 800 cm^{-1} and 1000 cm^{-1} due to the stretching vibration of Si-O-Si shows the dominance of silica and silica-based compounds at higher temperatures [153].

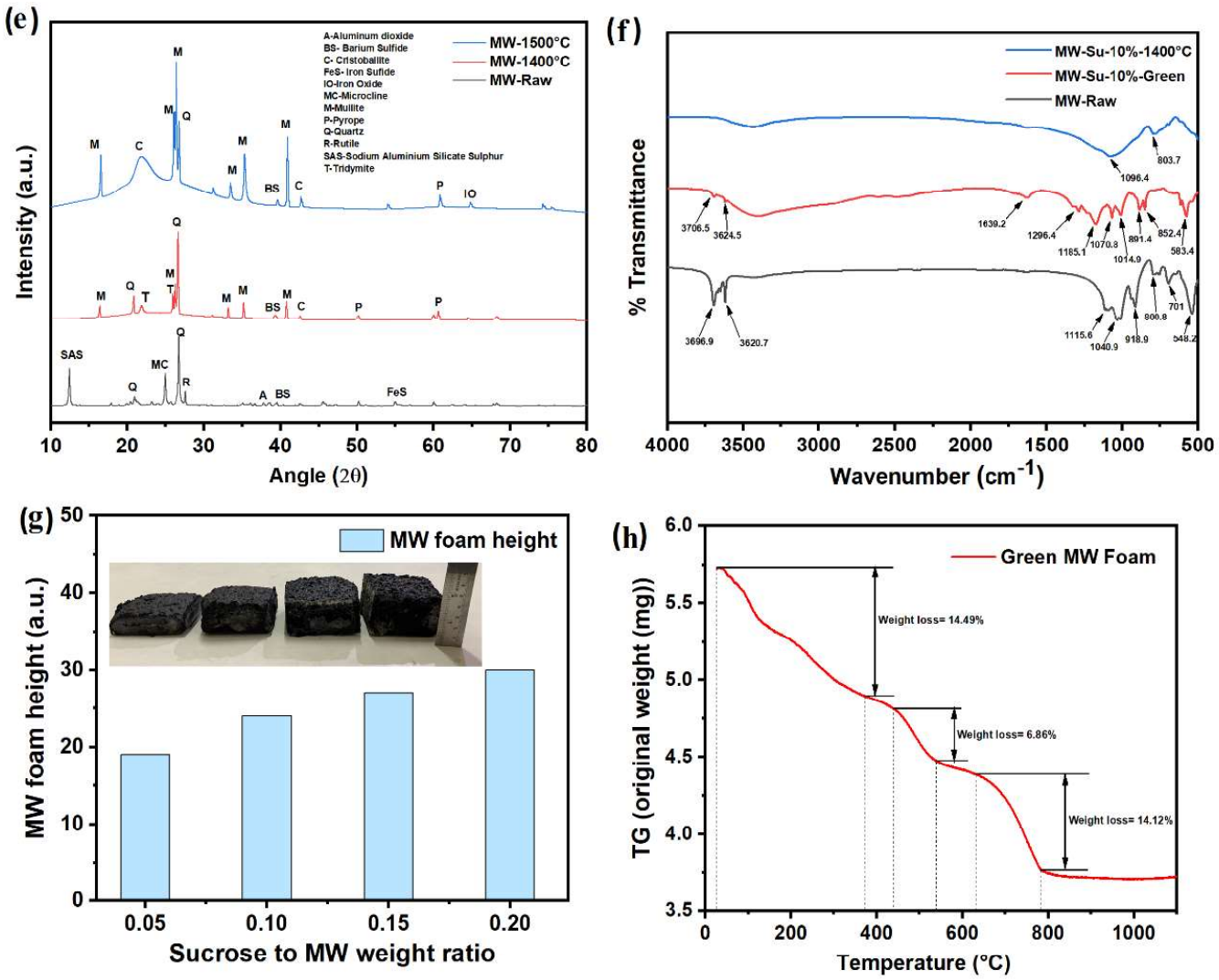

Fig. 6.2 (a) XRD analysis of raw MW and sintered FG-MS foam, (b) FTIR analysis of raw MW, Green MW foam and sintered FG-MS foam, (c) Foam height variation of Green FG-MS foam with $W_{Su/MW}$ ratio, (d) TGA analysis of Green MG-MS foam

Sintering causes the transformation of various mineralogical phases of raw MW into new phases. The mineralogical examination results revealed that most of the aluminosilicate minerals of raw MW undergo phase transformation and are predominantly mullite phase [JCPDS No.- 79-1457]. However, the percentage of mullite phase is high in samples sintered at 1500°C, showing better mullitization. Moreover, due to higher content of silicate minerals, silica is second most compound found in the sintered samples in their various forms. Presence of silica as quartz [JCPDS No.- 77-0126] is reduced in sintered samples due to mullitization

and conversion of quartz to tridymite [JCPDS No.- 79-1457] and cristobalite phase [JCPDS No.- 82-1233]. Iron sulphide [76-0964] which is assumed to be major factor of acid drainage is found to be reduced or diminished due to thermal decomposition of Iron sulphide and formation of Iron oxide [JCPDS No.- 84-0309] at higher temperatures. However, presence of barium sulphide [JCPDS No.- 30-0158]and sodium sulphide is still a concern for the acid drainage issue. Remaining phases which have their existence at higher temperatures are oxides of Sodium (Microcline) [JCPDS No.- 83-1604] and other metal oxides. Complexes of Magnesium (Pyrope) [81-0533] and Calcium (Titanite) with silicates are also found in small proportions. Formation of these complexes with rare earth elements (REE) and other elements are found to be helpful in reducing the amount of leachate of these elements. Leaching behaviour was assessed utilising the toxicity characteristic leaching approach (TCLP) to look at the mobility of heavy metals in the sintered MW foam. After dilution with 1N HCL solution, it was discovered that the pH of raw MW was less than 5, so the TCLP test was conducted using extraction solution 1 (pH = 4.93 ± 0.05), which had a solid-liquid ratio of 1:20. Table 6.2 lists the outcomes of heavy metals mobility. All thermally treated samples showed a considerable decrease in the mobility of heavy metal elements, which is confirmed to be within US-EPA regulation limits for non-hazardous waste.

The optical images shown in Fig 6.3(c) of sintered mullite-silica foam exhibit a typical porous structure with a 3D reticulated structure having open channels, which are also surrounded by some small and large-sized closed spherical cells as a blockage to open channels. The image shows side face of a cuboidal-shaped mullite-silicate foam, clearly depicting the gradient foaming effect showing gradient pore morphology, i.e., small pores near the bottom zone and comparatively larger pores at the top zone of the foam. The gradient in foaming or difference in pore size of FG-MS foam from bottom to top can be attributed to more gravity sustained by the relatively bottom portion of the MW slurry during foaming. The slurry at the bottom has a higher load than the slurry at the top side due to the self-weight of the MW slurry, which gives more resistance to escaping gases while foaming, thus not giving enough room to pass through the slurry. The bottom slurry counters the force exerted by escaping gases due to their self-weight, which causes less foaming of the slurry near the bottom side. As the escaping gases approach the top side of the slurry, relatively less resistance is realized due to less weight force offered by the top side slurry. This causes a gradient in the foaming phenomenon in green MW foamed samples which are further inherited in sintered samples. The images of the top and bottom surfaces delineate the above phenomenon showing less dense large macro pores at the

top and highly dense, relatively fine pores at the bottom of FG-MS foam. For more visualization and quantification, pores size at different layers of side face of FG-MS foam was measured. It was found that the average pore size at bottom zone was 36.84 µm while middle and top zone were 62.19 µm and 74.89 µm respectively, clearly showing increase in pore diameter with height. The accompanying graph shows gradual increase in pore size from bottom to top of FG-MS foam (Fig. 6.3(d)).

Table 6.1 Environmental and durability properties of selected MG-MS foam (TCLP test)

Samples/Elements	As μgL^{-1}	Ba μgL^{-1}	Cd μgL^{-1}	Cr μgL^{-1}	Cu μgL^{-1}	Mo μgL^{-1}	Pb μgL^{-1}	Sulfates μgL^{-1}	Zn μgL^{-1}
Raw MW	557	157	2.8	27.4	98	17.1	72.54	333.5	1247
FG-MS Foam	96	39	0.11	8.08	56	6.32	15.85	101.4	369

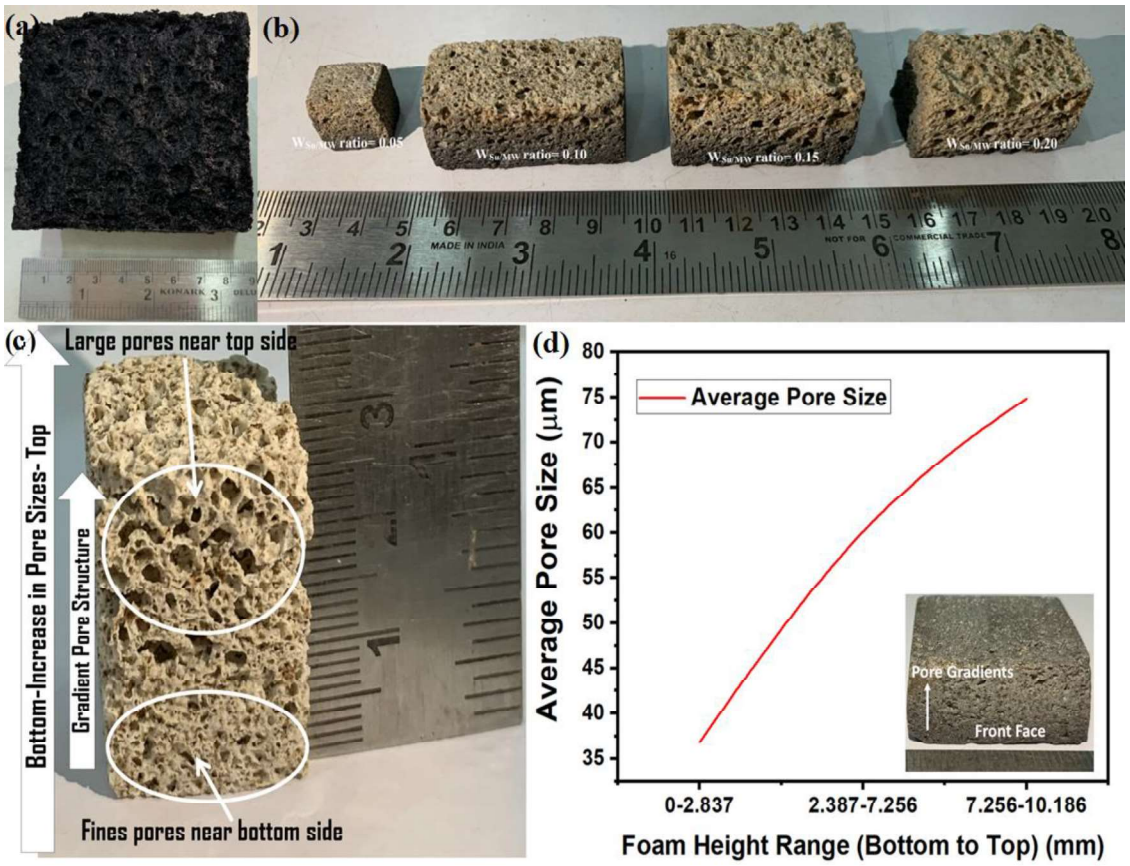

Fig. 6.3 (a) Green FG-MS foam (at 0.1 $W_{Su/MW}$ ratio), (b)Sintered FG-MS foam prepared with different $W_{Su/MW}$ ratio (0.05 to 0.2), (c) FG-MS foam showing gradient pore structure, (d) FG-MS foam showing pore size distribution at each face (sintered at 1400°C and prepared with 0.1 $W_{Su/MW}$ ratio)

Furthermore, to investigate more details of microstructure of FG-MS foam, SEM microphotographs have been examined. Fig 6.4 shows the SEM microstructure of top face (Fig. 6.4 (a)), bottom face (Fig. 6.4 (c)) and side face (Fig. 6.4 (d, e, f)) of the FG-MS foam (Fig. 6.4 (b)). The side face of foam is divided into three zones according to the pore size distribution. The bottom zone contains small pores most of which are closed one, as shown in SEM image (Fig. 6.4 (f)). The middle zone is transient phase where both closed and open pores are found with pore size comparatively larger than bottom zone pores (Fig. 6.4 (e)). Finally, the topmost zone comes where mostly larger and open pores are present (Fig. 6.4 (d)). The SEM images of these three zones of side face of foam clearly suggests that there is gradient in pore sizes from bottom to top. It is also demonstrated in SEM images of top and bottom surfaces of foam which has comparatively larger and open pores at top surface than bottom surface.

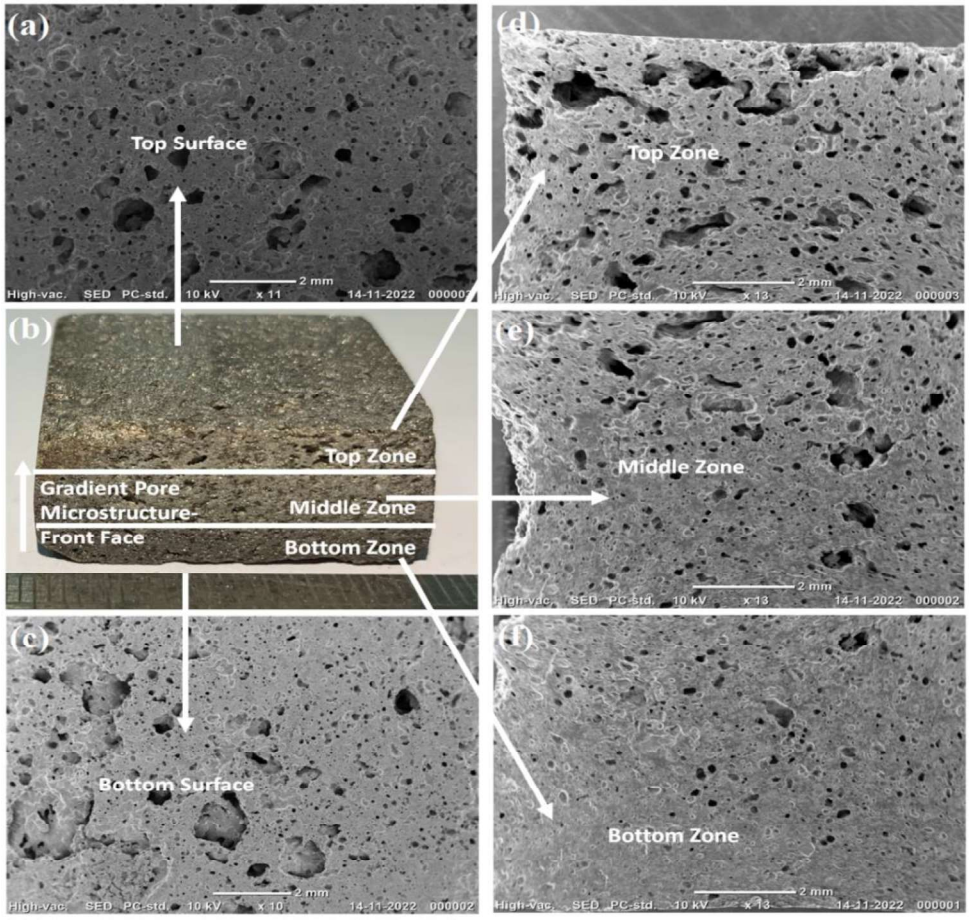

Fig. 6.4 FG-MS foam sintered at 1300°C and prepared at $W_{Su/MW}$ of 0.05 (b) with their corresponding SEM microstructure of (a) Top surface, (c) Bottom surface; (d) Topmost, (e) Middle, and (f) Bottom zone of side face

Fig 6.5 shows the SEM microstructure of the inner-cross-section of FG-MS foams prepared at different $W_{Su/MW}$ ratios and sintering temperatures, along with the EDS analysis and pore size distribution graphs. The developed foams exhibit both open and closed cells, demonstrating a typical microstructure prepared through the foaming method. The open pores found on each sample are relatively large and are in the macro range or more. These open pores provide a connected 3D network to MW foams, making them an excellent material for filter and acoustic applications.

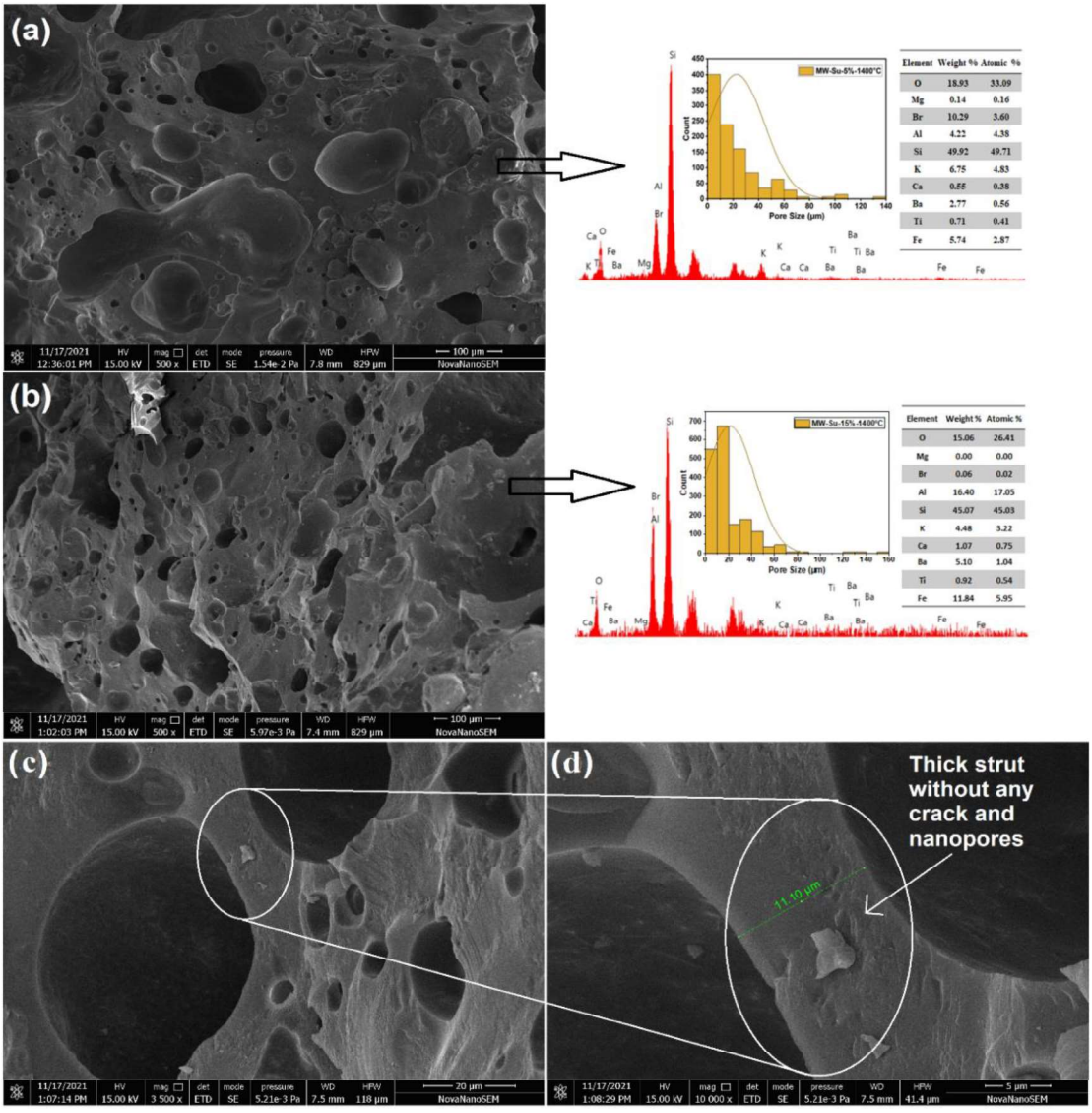

Fig. 6.5 SEM microstructure of FG-MS foams sintered at 1400°C and prepared at $W_{Su/MW}$ of (a) 0.05 (b) 0.15 with their corresponding high magnification SEM images and pore size distribution along with EDX analysis, (c, d) FG-MS foam demonstrating thick struts (0.1 $W_{Su/MW}$ ratio, 1400°C)

Closed pores are comparatively finer in size and are densely populated. Closed pores result from the removal of agglutinated carbon from the surfaces of MW particles or due to pressure exerted by relatively low-pressure escaping gases. It is found that the density of pores is increased with $W_{Su/MW}$ ratio, suggesting that the addition of sucrose promotes the transformation of large pores to small pores (closed). However, this is not true for open pores, which increases due to the increase in $W_{Su/MW}$ ratio. The reason for the above anomaly can be found in the formation of excess pressure inside the slurry due to high sucrose amount, which causes escaping gases to exert more pressure inside slurry, thereby increasing foam structure and size of open pores. Samples sintered at higher temperature shows similar pore morphology and a similar pattern of pore architecture with $W_{Su/MW}$ ratio variation. Pore size distribution of closed pores was analysed statistically using SEM images (at least five images of each composition) and results are shown with the respective SEM micrograph. It is discovered that the closed pores that FG-MS foams possess are micropores. When $W_{Su/MW}$ ratio is 0.05, the average pore size of FG-MS foams sintered at 1400°C is roughly 22.659 μm, but when this ratio is increased to 0.15, the average pore size drops to 21.175 μm. In contrast, when the sintering temperature is raised to 1500°C, an increase in average pore size is seen. When sintered at 1500°C with a $W_{Su/MW}$ ratio of 0.1, the mean pore width rises to 49.005 μm. The EDS analysis results demonstrate the presence of all potential components in the FG-MS foam, which are also attached to the SEM image. EDS results are in accordance with XRD and FTIR results, showing the presence of Fe, Al, Si, Ba, O, Ti and Ca elements, which confirms the existence of aluminosilicate and heavy metal-based oxides and mullite phase in FG-MS foam.

6.3.3 Physical and Thermo-Mechanical Properties of FG-MS Foam with Comparative and Cost Analysis

Physical properties of FG-MS foams prepared with different compositions are listed in Table 6.2. The obtained FG-MS foams have a bulk density in the range of 0.312-1.339 g/cm^3. Fig 6.6 shows the effect of $W_{Su/MW}$ ratio and sintering temperature on physico-mechanical properties of FG-MS foam. It is found that $W_{Su/MW}$ ratio has a significant effect on porosity level compared to sintering temperature. Approximately 30-35% increase in total porosity is observed for each composition with a 15% increase of sucrose amount while around 10 % variation is seen for a 200°C change in temperature (higher temperature between 1300°C-1500°C). Fig. 6.6 (a) shows the variation of total porosity and water absorption of FG-MS foam with $W_{Su/MW}$ ratio and is found to be varied linearly. As obvious, an increase in temperature decreases the porosity due to consolidation of pores at higher temperature. Total porosity and water retention capacity of

FG-MS foams are found to be in the range of 55-90% and 40-60% respectively. Water absorption capacity increases with $W_{Su/MW}$ ratio and remains constant after achieving a maximum value at 0.15 $W_{Su/MW}$ ratio. The reason for above can be found in the graph of open and closed pores (Fig. 6.6(b)) which clearly depicts that open porosity is constant in between 0.15-0.2 $W_{Su/MW}$ ratio. Open and closed porosity varies inversely up to 0.15 $W_{Su/MW}$ ratio and remains constant afterwards. Shrinkage is more for higher porous material and at higher temperatures (Fig. 6.6(c)). In spite of the fact that sintering at higher temperatures reduces porosity and increases linear shrinkage, sintering also provides strength to the structure. Ceramic foams of porosity greater than 80% are found to have low strength. Fig 6.6(d) shows the variation of compressive strength of the FG-MS foam with $W_{Su/MW}$ ratio and sintering temperature. Increase in $W_{Su/MW}$ ratio decreases compressive strength due to increase in porosity while increase in sintering temperature increases the strength. The developed FG-MS foam possesses compressive strength between 2.2-13.8 MPa. This notable compressive strength can be attributed to the presence of dense struts without cracks or nano-pores, as depicted in Figure 6.5 (c, d). Additionally, the mechanical strength of the FG-MS foams is enhanced by the formation of aluminosilicate phases, including mullite, as indicated by XRD analysis. Mullite, with its unique structure, exhibits higher strength and toughness compared to pure alumina and silica composites. The formation of the mullite phase is facilitated by higher temperature treatment, which promotes the reaction between alumina and silica, resulting in the formation of mullite.

Thermal conductivity of the as-fabricated FG-MS foam is plotted in Fig.6 (a). It is found that the fabricated FG-MS foam exhibit low thermal conductivity of 0.084 W/(m·K), in spite of the fact that mullite and silica themselves possesses high thermal conductivity of around 5.2 and 1.5 W/(m·K) respectively. The reason behind this can be due to relatively lower thermal conductivity of air which is entrapped inside the pores of FG-MS foam, providing extra resistance to heat flow. It is observed that the thermal conductivity decreases evidently as $W_{Su/MW}$ ratio increases from 0.05 to 0.2. Moreover, increase in sintering temperature from 1300°C to 1500°C, further enhancement of the thermal conductivity occurred due to the decrease in porosity. The thermal conductivity of fabricated FG-MS foam using sucrose dehydration process is compared with some of the existing mullite-based foams prepared through various routes and found to have better thermal resisting properties (Fig. 6.7(b)) [3–5,160,166–172].

Table 6.2 Different Mixture Compositions, the Corresponding Microstructural Properties of FG-MS foams Fabricated Using Sucrose Dehydration Process

Sucrose to MW weight ratio	Sintering Temperature (°C)	Bulk Density of Sintered FG-MS foam (g/cm^3)	Total Porosity (%)	Open Porosity (%)	Closed Porosity (%)	Water Absorption (%)
0.05	1300°C	1.11111	63.69269	15.11111	48.58158	10.198
0.10	1300°C	0.69564	77.26884	37.98799	39.28086	33.354
0.15	1300°C	0.48457	84.1659	50.36016	33.80574	60.247
0.20	1300°C	0.31175	89.81294	52.33157	37.48136	61.875
0.05	1400°C	1.21224	60.38794	13.82857	46.55937	9.6414
0.10	1400°C	0.81754	73.28537	33.27273	40.01264	31.479
0.15	1400°C	0.58895	80.75498	48.92086	31.83412	59.130
0.20	1400°C	0.45894	85.00321	50.55136	34.45185	60.866
0.05	1500°C	1.33888	56.24967	11.885	44.36467	8.956
0.10	1500°C	0.94549	69.10443	30.2564	38.84803	29.845
0.15	1500°C	0.64515	78.91859	45.98765	32.93093	53.234
0.20	1500°C	0.51986	83.01248	48.02546	34.98702	54.247

Several theories have been proposed to better predict the thermal conductivity of porous materials. Most of the models are developed on five basic structural models; specifically, the Parallel (PM), Series (SM), Effective Medium Theory (EMT) and Maxwell–Eucken (two forms (ME1 & ME2)) models. The thermal conductivity of FG-MS foam having hierarchical pore structures is predicted using the above-mentioned basic models along with Gong equation (Li et al., 2022) which provides the integrated equation of five basic effective thermal conductivity models (SM, PM, ME1, ME2, and EMT). Thermal conductivity of air, silica and mullite at ambient conditions is considered as 0.026, 1.5 and 5.2 W/(m·K) respectively. The thermal conductivity was calculated using aforementioned different theoretical models and compared with experimental data. To estimate the thermal conductivity of foams theoretically, the thermal conductivity of solid part of foam is taken 3.35 W/(m·K) (based on the assumption that the solid part of foam consists of equal portions of silica and mullite phase and ignoring other phases) while voids are assumed to be filled with air and thermal conductivity is assumed as 0.026 W/(m·K). The estimated results (shown in Fig. 6.7(c, d)) reveal that thermal conductivity values are quite different obtained with various models and the experimental values agree with certain models within specific porosity ranges. In the porosity range of 50-

70 %, ME 2 shows best result with a difference of 58-70% followed by SM, EMT and GE models. However, in the porosity range of 80-90%, EMT shows best-predicted value followed by ME 2, SM and GE models. Overall, in the wide porosity range, the experimental results were closer to the data calculated by the ME 2 model and are in good agreement with it. Therefore, the ME 2 equation is best-suited model for predicting and evaluating thermal conductivity of FG-MS foam fabricated via sucrose dehydration process at ambient temperature.

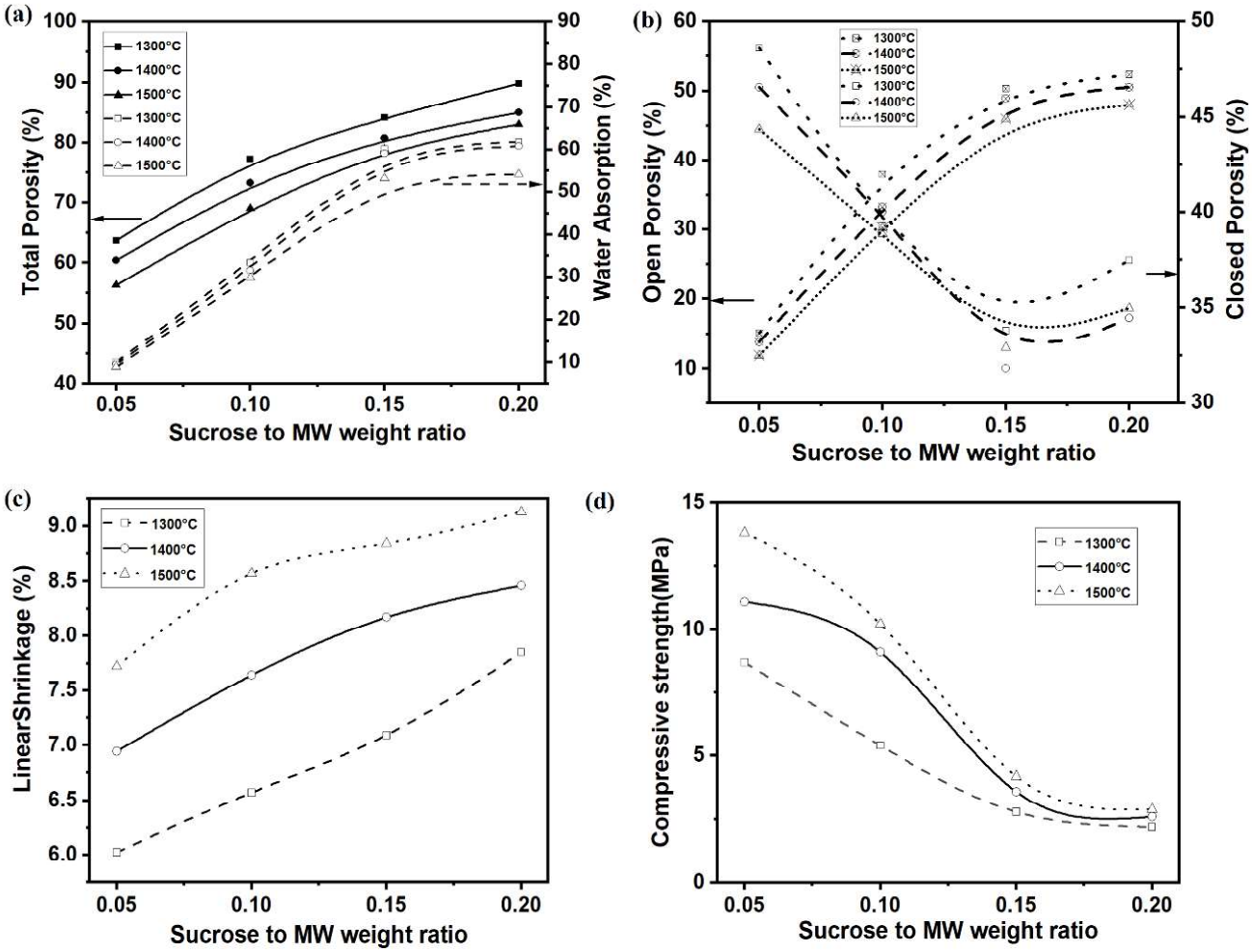

Fig. 6.6 Variation of (a) Total porosity, (b) Open and Closed pores, (c) Linear shrinkage, (d) Compressive strength of FG-MS foams with sucrose to MW weight ratio.

The price of the raw materials used to create a 10*10*10 cm^3 MW foam is broken down in detail in Table 4. The price of the raw materials to produce the required quantity of MW foam is around ₹ 1.22. Green synthesis and sintering at 1400°C will cost approximately ₹ 48/sample. The above dehydration process is a cost-effective solution towards a successful waste

valorisation pathway for aluminosilicate-rich solid waste, with a total estimated cost of developed MW foam of roughly ₹ 49.22/sample ($0.595).

Table 6.3 Cost analysis of the developed MW derived FG-MS foam

Raw materials	Unit price (₹/kg)	Amount used per FG-MS Foam [10*10 *10 cm^3] (g)	Cost per FG-MS foam (₹)
MW Powder (based on transportation, ball milling and handling charges)	2	95	0.19
Sucrose	38	5	0.19
Sulphuric Acid (98 %)	14	60	0.84
Total raw material cost per FG-MS foam			₹1.22
Approximate cost of shaping and sintering at 1400°C for 2 h (based on the power rating of the furnace and unit electricity price).			₹48/sample
Estimated total cost			$0.595/sample
*Currency conversion used (USD to INR): $1 = ₹82.75.			

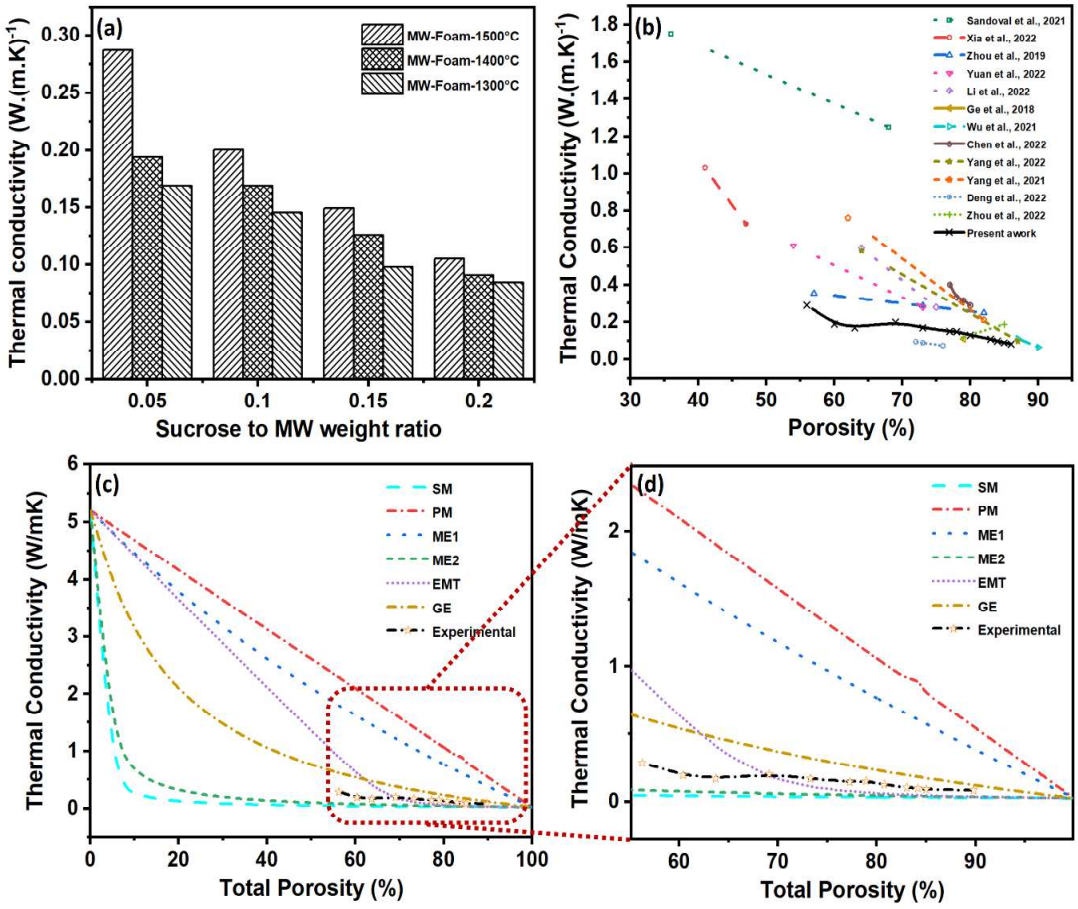

Fig. 6.7 Variation of (a) Thermal Conductivity variation of FG-MS foam with $W_{Su/MW}$ ratio at different temperatures, (b) Comparative analysis of Thermal conductivities, (c, d) Predicted thermal conductivity of FG-MS foam with different models.

6.4 Conclusions

The present work is an effort to reduce the environmental impact of solid waste, rich in aluminosilicate minerals by utilizing and converting it into a high-end value product. Highly porous mullite-silicate foam with gradient microstructure has been successfully fabricated through a facile, inexpensive and adaptable approach by efficiently utilizing MW. The results show that foam with gradient pore structure having uniform pore morphology can be achieved by this technique. High aluminosilicate components in raw MW and sintering of green MW foam at high temperature favours the formation of mullite phase. The fabricated FG-MS foams are found to have bulk density, porosity and compressive strength in the range of 0.31-1.34 g/cm^3, 56.25-89.81% and 2.97-13.8 MPa respectively. Results demonstrate that FG-MS foams have good thermal resistivity properties with low thermal conductivity up to 0.08 W/(m·K) which is better than reported thermal insulation properties of other mullite-based material systems. Overall, the above-mentioned process is a promising technology as a means of low-cost way to recycle heterogeneous and hazardous coal mine overburden waste to useful highly porous ceramic foams. The developed ceramic foam due to its favourable thermoelastic properties can find industrial applications as filters, thermal insulators, adsorbent and refractory material. In addition, the current approach could become an efficient and cost-effective method for recycling aluminosilicate-based industrial waste into mullite composite foams, following the concept of circular economy and sustainable development.